Energy-efficient trajectory planning and resource allocation in UAV communication networks under imperfect channel prediction

Min SHENG, Chenxi ZHAO*, Junyu LIU, Wei TENG, Yanpeng DAI & Jiandong LI

State Key Laboratory of ISN, Xidian University, Xi'an 710071, China

Abstract In unmanned aerial vehicle (UAV) communication networks, trajectory planning and resource allocation (TPRA) under channel prediction obtains great attention due to its significant energy-saving of UAVs and user quality of service (QoS) gains. These potentials are primarily demonstrated under the assumption of perfect channel prediction. However, due to the rapid-varying features of air-to-ground channels, it is difficult to avoid the random channel prediction error (CPE), which may deteriorate the performance of TPRA. In this paper, we investigate the problem of energy-efficient TPRA considering random CPE. The problem is formulated as a mixed-integer non-convex optimization with chance constraints, which ensures that QoS is robust to random CPE. To solve it, we first transform the chance constraints into deterministic forms, which are further proved to be convex constraints by using the characteristic of quasiconvex functions. Then, we design a modified successive convex approximation algorithm to iteratively achieve the optimal solution. To cater to the high-speed movement of UAVs, a low-complexity heuristic online algorithm is tailored. Specifically, we first relax the QoS constraints to find a feasible initial point and iteratively tighten the lower bound of QoS constraints to obtain a suboptimal solution. Simulation results show that the proposed algorithm can improve energy efficiency compared with the algorithm without prediction.

Keywords UAV communication networks, trajectory planning, resource allocation, channel prediction

1 Introduction

To provide ubiquitous communication services, aerial base stations (ABSs) based on unmanned aerial vehicles (UAVs) are proposed as a promising method to complete fast and flexible deployment of communication systems [1–4]. Due to the high mobility, the UAV trajectory and communication resource can be designed according to the real-time wireless environment and demands of ground users (GUs), which introduces spatial degrees of freedom for providing a higher quality of service (QoS). Despite the potential benefits, it is challenging to design the algorithm of trajectory planning and resource allocation (TPRA) in UAV communication networks due to the high mobility of UAVs. On the one hand, the resource allocation policy is generally outdated due to the delay imposed by channel state information (CSI) collection and algorithm running. On the other hand, the perfect channel prediction is unrealistic since air-to-ground channels in high-mobility UAV networks are rapid-varying [5]. Worse still, the channel prediction error (CPE) is difficult to handle due to its randomness. Hence, to achieve efficient TPRA, it is important to overcome the impact of random CPE on system performance. In this paper, we focus on the robust TPRA under the imperfect channel prediction in UAV communication networks.

---

* Corresponding author (email: chenxizhao@stu.xidian.edu.cn)

info.scichina.com   link.springer.com

1.1 Related work

Compared with terrestrial communication networks, UAV trajectory optimization is a unique and fundamental problem in UAV communication networks. In [6], the trajectory and data collection policy is jointly designed in the low earth orbit satellite assisted-UAV networks to minimize the total energy consumption. The energy-efficient UAV communication with a ground terminal is studied via optimizing the UAV's trajectory [7]. In particular, the propulsion energy consumption model of the fixed-wing UAV is derived as a function of UAV's flying speed. Besides the trajectory planning, resource allocation also significantly impacts the system performance. In [8], researchers studied the UAV access selection and BS bandwidth allocation problems in a UAV-assisted IoT communication network, and proposed a hierarchical game framework. Considering both the orthogonal multiple access (OMA) and non-orthogonal multiple access (NOMA) modes, TPRA is investigated to maximize the minimum average rate of GUs for UAV communication networks [9]. In [10], the user communication scheduling, UAV trajectory, and resource allocation were jointly optimized to maximize energy-efficiency and satisfy quality of experience (QoE) requirements of users. Studies on TPRA are generally based on two widely used assumptions [6, 11–14], i.e., (1) the exact mathematical model of CSI is given in advance and changeless, (2) the time cost of CSI collection and algorithm running is ignored. However, the complete knowledge of CSI is generally unknown in UAV communication networks. Moreover, the delay imposed by CSI collection and algorithm running may invalidate the resource allocation policy. Therefore, channel prediction based methods should be studied for TPRA in UAV communication networks.

To effectively optimize TPRA and further improve the system performance, it is essential to predict CSI of the air-to-ground channel between UAV and GU. Aided by the channel prediction, the online TPRA is proposed and widely applied in UAV communication networks [15–17]. In [15], the shadow fading in a given environment was predicted by leveraging the Gaussian process, and then the relay trajectory is optimized by using the learned communication properties. In [16], a UAV was deployed to establish communication links between users and base stations. The relay deployment is optimized via online learning without prior knowledge of CSI. In [17], the 3D-trajectory planning and resource allocation were optimized through an online algorithm, which only requires real-time and statistical knowledge of CSI. In the literature above, CPE is not considered. However, in practice, the random CPE always exists and further may result in the waste of resources and violation of QoS constraints [5, 18]. Thus, it is necessary to research robust approaches to handle the random CPE and further avoid QoS violations in UAV communication networks.

As discussed above, TPRA with channel prediction is challenging in UAV communication networks. On the one hand, the exact prediction of CSI is of paramount importance for TPRA due to the high-mobility features of UAV communication networks. On the other hand, there is no such thing as a perfect channel prediction in UAV communication networks. The random CPE is a huge obstacle to satisfying QoS constraints of GUs.

1.2 Contributions

In this paper, we investigate TPRA under imperfect channel prediction in UAV communication networks. To handle the random CPE, we focus on how robustness can be incorporated into TPRA. An optimization framework is proposed, where the framework is robust to CPE that follows a Gaussian distribution model. The contributions of this paper are more specifically summarized below.

• We formulate a robust optimization problem to maximize the long-term expected energy efficiency according to the real-time channel prediction. Specifically, the QoS requirements of GUs are modeled as probabilistic chance constraints in which the CPE is a Gaussian random variable. Furthermore, we adopt a safe approximation to transform the probabilistic chance constraints into deterministic forms, which are proved to be convex constraints by using the characteristic of quasiconvex functions. Then, we obtain the optimal solution with a modified successive convex approximation (SCA) algorithm.

• To provide a real-time TPRA, we further propose a low-complexity online algorithm. In particular, we relax the initial QoS constraints since it is non-trivial to find a feasible initial point due to the coupling between trajectory planning and resource allocation. Then, we design a heuristic algorithm to improve the solution by iteratively tightening the lower bound of QoS constraints. Furthermore, simulation results show that the proposed algorithm can improve the energy efficiency compared with the algorithm without prediction.
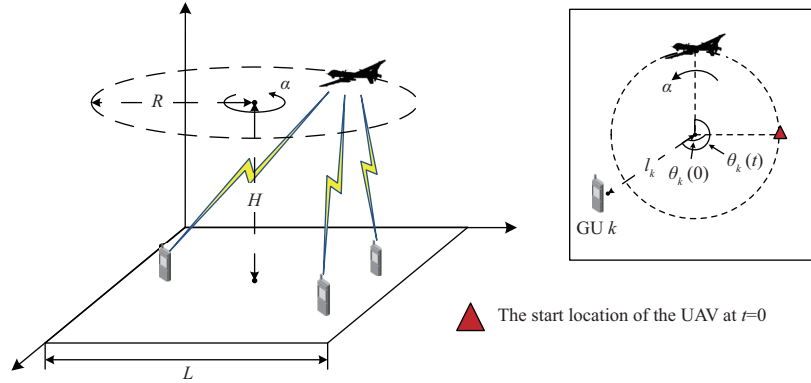
Figure 1 (Color online) The UAV network providing content service for GUs in a target region.

The rest of this paper is organized as follows. In Section 2, the system model of the UAV communication network is presented. The TPRA formulation with the perfect channel prediction is proposed in Section 3. In Section 4, the algorithm for the robust TPRA with random CPE is given. Simulation results are presented in Section 5, which is followed by the conclusion in Section 6.

2 System model

2.1 UAV communication system model

We consider a UAV communication system including one ABS mounted on UAV and K GUs, which are located in a squared target region with side length L (see Figure 1). Let $\mathcal{K} = (1, \ldots, K)$ denote the set of GUs. The hover center and hover radius of the fixed-wing UAV are denoted by $\boldsymbol{C} = (C_x, C_y)$ and R, respectively. In addition, the angular velocity of the fixed-wing UAV is denoted by α. Let $\boldsymbol{w}_k \in \mathbb{R}^2$ denote the horizontal coordinate of GU k. The flight duration T is divided into N_T equal-length time slots, where the duration of each time slot equals T_s such that $T = N_T T_s$. Note that the location of the UAV can be assumed to be unchanged during each time slot when T_s is chosen sufficiently small [7]. Let $\mathcal{T} = (0, \ldots, N_T)$ denote the set of time slots, and $\boldsymbol{u}(t) \in \mathbb{R}^2, \forall t \geqslant 0$ denote the horizontal trajectory coordinates of the UAV at time slot t. The distance between the UAV and GU k at time slot t is given by

$$d_k(R, t) = \sqrt{H^2 + \|\boldsymbol{u}(t) - \boldsymbol{w}_k\|^2}, \tag{1}$$

where H is the flight height of the UAV. Letting $\theta_k(t)$ denote the hover angle with respect to GU k at time slot t (see Figure 1), we have

$$\|\boldsymbol{u}(t) - \boldsymbol{w}_k\| = \sqrt{R^2 + l_k^2 + 2l_k R \sin(\theta_k(t))}, \tag{2}$$

where l_k is the horizontal distance from the UAV hover center to GU k (see Figure 1), i.e., $l_k = \sqrt{\|\boldsymbol{w}_k - \boldsymbol{C}\|^2}$. Furthermore, in (2), we have $\theta_k(t) = \theta_k(0) + \alpha t$.

All GUs share the same frequency band multiplexed in time domain. Specifically, system bandwidth W Hz is divided into N_{F} orthogonal subcarriers, and each subcarrier can be allocated to at most one GU in each time slot. Let $\mathcal{I} = (1, \ldots, N_{\mathrm{F}})$ denote the set of subcarriers. $s_{i,k}(t) \in \{0, 1\}$ is the binary subcarrier allocation indicator. Particularly, $s_{i,k}(t) = 1$ indicates that subcarrier i is allocated to GU k at time slot t and $s_{i,k}(t) = 0$, otherwise. Let $\boldsymbol{s}$ denote the subcarrier allocation policy vector.

Let $\mathcal{C} = \{1, 2, \ldots, C\}$ denote the set of contents. In this paper, rateless Fountain coding is applied, where each content is encoded into several different segments, and it can be recovered by collecting a certain number of encoded segments. Specifically, we consider that each content is encoded into multiple segments with size S bits, and a content can be recovered by collecting K encoded segments. Furthermore, we set the storage capacity for caching segments in each GU as $J = SKN_{\mathrm{C}}$ bits. In other words, each GU can cache the encoded segments of N_{C} contents. We assume that each GU sends its content requests to the UAV at the beginning of each flight cycle. If GU k cannot collect at least K encoded segments of the requested content s within a flight cycle, it will delete the received encoded segments of content s from its storage.

2.2 Channel model

Let P denote the transmit power from the UAV to GUs at each time slot. Therefore, at time slot t, assuming subcarrier i is allocated to GU k, the achievable transmission rate (bits/s) on subcarrier i is given by

$$r_{i,k}\left(t, \tilde{\rho}_{i,k}\left(t\right)\right) = B\log_2\left(1 + \frac{P\beta_0\rho_{i,k}\left(t\right)}{\left(d_k\left(R,t\right)\right)^2 N_0 B}\right),\tag{3}$$

where N_0 denotes the noise power spectral density and $B = W/N_{\mathrm{F}}$ is the bandwidth of each subcarrier. β_0 denotes the channel power gain at the reference distance. Moreover, we have $\rho_{i,k}\left(t\right) = \left|h_{i,k}\left(t\right)\right|^2$, where $h_{i,k}(t)$ is the channel coefficient that captures the shadow fading and small-scale fading effects due to multipath propagation.

In our early work [19], we found that the power gain of channels from the UAV to GUs has correlations in time domain. Thus, it is reasonable to design TPRA algorithm based on predicted CSI. In the considered UAV communication network, exact $d_k\left(t\right)$ can be obtained since the locations of GUs are known. Hence, the CPE mainly reflects in the predicted channel coefficient. Note that, in practice, the channel prediction generally only consists of the expectation and variance of channel coefficients rather than exact value [17]. Thus, in this paper, CPE is defined as the prediction error for the expectation and variance of the modular squaring of channel coefficient, i.e., $\rho_{i,k}\left(t\right)$. The CPE is generally caused by the fast time-varying wireless channel and the delay for collection of CSI. Let $\tilde{\rho}_{i,k}\left(t\right)$ denote the predicted value of $\rho_{i,k}\left(t\right)$, where $\mathbb{E}\left\{\tilde{\rho}_{i,k}\left(t\right)\right\}$ and $\mathbb{V}\left\{\tilde{\rho}_{i,k}\left(t\right)\right\}$ denote the expectation and variance of $\tilde{\rho}_{i,k}\left(t\right)$. Similarly, $\mathbb{E}\left\{\rho_{i,k}\left(t\right)\right\}$ and $\mathbb{V}\left\{\rho_{i,k}\left(t\right)\right\}$ denote the expectation and variance of $\rho_{i,k}\left(t\right)$. If $\mathbb{E}\left\{\tilde{\rho}_{i,k}\left(t\right)\right\} = \mathbb{E}\left\{\rho_{i,k}\left(t\right)\right\}$ and $\mathbb{V}\left\{\tilde{\rho}_{i,k}\left(t\right)\right\} = \mathbb{V}\left\{\rho_{i,k}\left(t\right)\right\}$, the CSI is exactly predicted. Thus, in this paper, CPE mainly reflects in the predicted error of $\mathbb{E}\left\{\rho_{i,k}\left(t\right)\right\}$ and $\mathbb{V}\left\{\rho_{i,k}\left(t\right)\right\}$. $\psi_{i,k}\left(t\right)$ denotes the prediction error of $\mathbb{E}\left\{\rho_{i,k}\left(t\right)\right\}$, i.e., $\psi_{i,k}\left(t\right) = \mathbb{E}\left\{\rho_{i,k}\left(t\right)\right\} - \mathbb{E}\left\{\tilde{\rho}_{i,k}\left(t\right)\right\}$. In this paper, $\psi_{i,k}\left(t\right)$ is modeled as a normal random variate with expectation $\mu_{i,k}\left(t\right)$ and variance $\sigma_{i,k}^2\left(t\right)$, i.e., $\psi_{i,k}\left(t\right) \sim \mathcal{N}(\mu_{i,k}\left(t\right), \sigma_{i,k}^2\left(t\right))$. Let $\Psi = \left(\psi_{i,k}\left(t\right), i \in \mathcal{I}, k \in \mathcal{K}, t \in \mathcal{T}\right)$ denote the vector of prediction errors. We assume that prediction errors are independent with each other. Thus, Ψ is a normal multivariate random vector with expectation $\boldsymbol{\mu} = \left(\mu_{i,k}\left(t\right), i \in \mathcal{I}, k \in \mathcal{K}, t \in \mathcal{T}\right)$ and variance $\boldsymbol{\sigma}$, where $\boldsymbol{\sigma} = \mathrm{diag}\{\sigma_{1,1}^2\left(1\right), \ldots, \sigma_{N_{\mathrm{F}},K}^2\left(N_T\right)\}$. In practice, if we know the biases of the channel predictions before the planning, we can adjust the predicted channels accordingly. Hence, in the following of this paper, we set $\mu_{i,k}\left(t\right) = 0, i \in \mathcal{I}, k \in \mathcal{K}, t \in \mathcal{T}$, i.e., $\psi_{i,k}\left(t\right) \sim \mathcal{N}(0, \sigma_{i,k}^2\left(t\right))$.

2.3 UAV energy model

The energy consumption of UAVs generally consists of computing energy, propulsion energy and transmission energy. In general, the propulsion energy is much larger than computing energy and transmission energy. Thus, in this paper, the computing energy and transmission energy are ignored. The total propulsion energy of the fixed-wing UAV is a function of velocity and acceleration [20]:

$$E\left(v\left(t\right)\right) = \int_0^T \left[a_1\left(v\left(t\right)\right)^3 + \frac{a_2}{v\left(t\right)}\left(1 + \frac{a\left(t\right)^2}{g^2}\right)\right]\mathrm{d}t + \frac{1}{2}m\left(\left(v\left(T\right)\right)^2 - \left(v\left(0\right)\right)^2\right),\tag{4}$$

where $v\left(t\right)$ and $a\left(t\right)$ are the velocity and acceleration of the UAV at time slot t, respectively. In addition, a_1 and a_2 are two parameters related to the aircraft's weight, wing area, air density and so on. g is the gravitational acceleration, and m is the mass of the UAV including all its payload. In this paper, the total propulsion consumption within each flight cycle can be rewritten as [21]

$$\begin{aligned}E\left(R\right) &= \left[\left(a_1 + \frac{a_2}{g^2 R^2}\right)\left(\alpha R\right)^3 + \frac{a_2}{\alpha R}\right]T_{\mathrm{s}}N_T\\ &= \left(a_1\alpha^3 R^3 + \frac{a_2\alpha^3}{g^2}R + \frac{a_2}{\alpha R}\right)T_{\mathrm{s}}N_T.\end{aligned}\tag{5}$$

Specifically, since the UAV flies at a constant angular velocity α and hover radius R, we have $\left(v\left(T\right)\right)^2 - \left(v\left(0\right)\right)^2 = 0$ in (4).

3 TPRA under perfect prediction

In this section, we first define the adopted performance metric, and then, we formulate the TPRA problem considering perfect prediction of channel coefficients.

3.1 Quality of service for GUs

In this paper, we assume that the QoS of a GU is satisfied when the GU can successfully receive at least N_{Q} requested contents within a flight cycle. Thus, the QoS constraints of GUs can be given by

$$\sum_{t\in\mathcal{T}}\sum_{i\in\mathcal{C}}s_{i,k}\left(t\right)T_{\mathrm{s}}r_{i,k}\left(t,\tilde{\rho}_{i,k}\left(t\right)\right)\geqslant N_{\mathrm{Q}}SK,\quad\forall k\in\mathcal{K}. \tag{6}$$

Note that the left hand side of (6) is the expected data received by GU k according to the predicted channel coefficient $\tilde{\rho}_{i,k}\left(t\right)$.

3.2 Optimization problem formulation

In this paper, we maximize the energy efficiency under the QoS constraints of GUs within each flight cycle. The TPRA problem is formulated as the following optimal programming:

$$(\mathrm{P0})\quad\max_{R,\boldsymbol{s}}\frac{1}{E\left(R\right)}\sum_{t\in\mathcal{T}}\sum_{i\in\mathcal{I}}\sum_{k\in\mathcal{K}}s_{i,k}\left(t\right)T_{\mathrm{s}}r_{i,k}\left(t,\tilde{\rho}_{i,k}\left(t\right)\right)$$

$$\mathrm{s.t.}\ \mathrm{C1}:\sum_{t\in\mathcal{T}}\sum_{i\in\mathcal{I}}s_{i,k}\left(t\right)T_{\mathrm{s}}r_{i,k}\left(t,\tilde{\rho}_{i,k}\left(t\right)\right)\geqslant N_{\mathrm{Q}}SK,\ \forall k\in\mathcal{K},$$

$$\mathrm{C2}:\sum_{k\in\mathcal{K}}s_{i,k}\left(t\right)\leqslant1,\ \forall i\in\mathcal{I},\ t\in\mathcal{T},$$

$$\mathrm{C3}:\sum_{i\in\mathcal{I}}s_{i,k}\left(t\right)\geqslant1,\ \forall k\in\mathcal{K},\ t\in\mathcal{T},$$

$$\mathrm{C4}:s_{i,k}\left(t\right)\in\left\{0,1\right\},\ \forall i\in\mathcal{I},\ t\in\mathcal{T},k\in\mathcal{K},$$

$$\mathrm{C5}:R_{\mathrm{min}}\leqslant R\leqslant R_{\mathrm{max}}.$$

The objective function is to maximize the energy efficiency of the UAV communication system, where the numerator is the total data received by all GUs during each flight cycle, which is a function with respect to the resource allocation policy and hover radius. Constraint C1 is the QoS constraint of each GU. Specifically, the QoS of a GU is satisfied when the GU can successfully receive at least N_{Q} requested contents within a flight cycle. Therefore, the QoS of a GU is satisfied if the GU can receive at least $N_{\mathrm{Q}}SK$ bits within a flight cycle. Constraints C2 and C4 are imposed to guarantee that each subcarrier is allocated to at most one GU at each time slot. Constraints C3 and C4 are imposed to guarantee that each GU should occupy at least one subcarrier at each time slot. Constraint C5 restricts the hover radius R.

Note that the solution of problem (P0) is an offline TPRA policy, where the value of channel coefficients should be exactly obtained. However, in practice, despite machine learning and data mining techniques, the channel prediction generally only consists of the expectation and variance of channel coefficients rather than the exact value. In this case, the expectation of transmitted data is used as the system performance metric. Considering the running time of algorithm, we formulate the online TPRA optimization problem as

$$(\mathrm{P1})\quad\max_{R,\boldsymbol{s}}\frac{1}{E\left(R\right)}\left(\sum_{k\in\mathcal{K}}A_{k,t_0}+\sum_{t\in\mathcal{T}_{t_0}}\sum_{i\in\mathcal{I}}\sum_{k\in\mathcal{K}}H_{i,k}\left(\tilde{\rho}_{i,k}^{t_0}\left(t\right)\right)\right)$$

$$\mathrm{s.t.}\ \mathrm{C1a}:A_{k,t_0}+\sum_{t\in\mathcal{T}_{t_0}}\sum_{i\in\mathcal{I}}H_{i,k}\left(\tilde{\rho}_{i,k}^{t_0}\left(t\right)\right)\geqslant N_{\mathrm{Q}}SK,\ \forall k\in\mathcal{K},$$

$$\mathrm{C2}\text{–}\mathrm{C5}.$$

In problem (P1), t_0 is the index of the current time slot, where $1 \leqslant t_0 \leqslant N_T - T_E$, and $\mathcal{T}_{t_0} = \{t_0 + T_E, \ldots, N_T\}$ with T_E denoting the algorithm running time. A_{k,t_0} is the total number of bits received by GU k until time slot $t_0 + T_E - 1$, which is given by

$$A_{k,t_0} = \sum_{t \in \mathcal{T} \setminus \mathcal{T}_{t_0}} \sum_{i \in \mathcal{I}} \hat{s}_{i,k}(t) T_s r_{i,k}(t, \hat{\rho}_{i,k}(t)). \tag{7}$$

In (7), $\hat{s}_{i,k}(t)$ is the subcarrier allocation policy for time slot t, $0 \leqslant t \leqslant t_0 + T_E - 1$, which has been already optimized before time slot t_0. Moreover, $\hat{\rho}_{i,k}(t)$ is the real channel coefficient if channel i is allocated to GU k at time slot t. Furthermore, $\tilde{\rho}_{i,k}^{t_0}(t)$ is the prediction of $\rho_{i,k}(t)$ at time slot t_0, and $\tilde{\boldsymbol{\rho}}_{t_0} = \{\tilde{\rho}_{i,k}^{t_0}(t), \forall i \in \mathcal{I}, k \in \mathcal{K}, t \in \mathcal{T}_{t_0}\}$. Accordingly, in problem (P1), $H_{i,k}(t, \tilde{\rho}_{i,k}^{t_0}(t))$ is the predicted channel transmission rate of channel i from the UAV to GU k at time slot $t, \forall t \in \mathcal{T}_{t_0}$, where we have

$$H_{i,k}\left(t, \tilde{\rho}_{i,k}^{t_0}(t)\right) = \mathbb{E}\left\{s_{i,k}(t) T_s B \log_2\left(1 + \tilde{\rho}_{i,k}^{t_0}(t) C\left(d_k(R,t)\right)^{-2}\right)\right\} \tag{8}$$

with $C = \frac{P\beta_0}{N_0 B}$. Note that the online algorithm for TPRA programming problem in (P1) should be performed in each time slot. For facilitating a tractable TPRA algorithm design, we rewrite (8) as [17]

$$
\begin{aligned}
&H_{i,k}\left(t, \tilde{\rho}_{i,k}^{t_0}(t)\right) \\
&\overset{(a)}{=} s_{i,k}(t) T_s B \mathbb{E}\left\{\log_2\left(1 + \mathbb{E}\left\{\tilde{\rho}_{i,k}^{t_0}(t)\right\} C\left(d_k(R,t)\right)^{-2}\right) + \frac{(\tilde{\rho}_{i,k}^{t_0}(t) - \mathbb{E}\{\tilde{\rho}_{i,k}^{t_0}(t)\}) C\left(d_k(R,t)\right)^{-2}}{(1 + \mathbb{E}\{\tilde{\rho}_{i,k}^{t_0}(t)\} C\left(d_k(R,t)\right)^{-2}) \ln 2} \right. \\
&\quad \left. - \frac{(C\left(d_k(R,t)\right)^{-2})^2(\tilde{\rho}_{i,k}^{t_0}(t) - \mathbb{E}\{\tilde{\rho}_{i,k}^{t_0}(t)\})^2}{(2\ln 2)(1 + \mathbb{E}\{\tilde{\rho}_{i,k}^{t_0}(t)\} C\left(d_k(R,t)\right)^{-2})^2} + o\right\} \\
&= s_{i,k}(t) T_s B \left[\log_2\left(1 + \mathbb{E}\left\{\tilde{\rho}_{i,k}^{t_0}(t)\right\} C\left(d_k(R,t)\right)^{-2}\right) + \frac{(\mathbb{E}\{\tilde{\rho}_{i,k}^{t_0}(t)\} - \mathbb{E}\{\tilde{\rho}_{i,k}^{t_0}(t)\}) C\left(d_k(R,t)\right)^{-2}}{(1 + \mathbb{E}\{\tilde{\rho}_{i,k}^{t_0}(t)\} C\left(d_k(R,t)\right)^{-2}) \ln 2} \right. \\
&\quad \left. - \frac{(C\left(d_k(R,t)\right)^{-2})^2(\mathbb{E}\{(\tilde{\rho}_{i,k}^{t_0}(t))^2\} - 2\mathbb{E}\{\tilde{\rho}_{i,k}^{t_0}(t)\}\mathbb{E}\{\tilde{\rho}_{i,k}^{t_0}(t)\} + (\mathbb{E}\{\tilde{\rho}_{i,k}^{t_0}(t)\})^2)}{(2\ln 2)(1 + \mathbb{E}\{\tilde{\rho}_{i,k}^{t_0}(t)\} C\left(d_k(R,t)\right)^{-2})^2} + o\right] \\
&= s_{i,k}(t) T_s B \left[\log_2\left(1 + \mathbb{E}\left\{\tilde{\rho}_{i,k}^{t_0}(t)\right\} C\left(d_k(R,t)\right)^{-2}\right) - \frac{(C\left(d_k(R,t)\right)^{-2})^2 \mathrm{Var}\{\tilde{\rho}_{i,k}^{t_0}(t)\}}{(2\ln 2)(1 + \mathbb{E}\{\tilde{\rho}_{i,k}^{t_0}(t)\} C\left(d_k(R,t)\right)^{-2})^2} + o\right],
\end{aligned}
\tag{9}
$$

where (a) is due to the second-order Taylor series expansion of $\log_2(1 + \tilde{\rho}_{i,k}^{t_0}(t) C\left(d_k(R,t)\right)^{-2})$ around $\mathbb{E}\{\tilde{\rho}_{i,k}^{t_0}(t)\}$, and o is the higher-order infinitesimal terms.

Furthermore, in UAV communication systems, $\mathbb{E}\{\tilde{\rho}_{i,k}^{t_0}(t)\} \gg \mathrm{Var}\{\tilde{\rho}_{i,k}^{t_0}(t)\}$ holds in general since the line-of-sight (LoS) path dominates in air-to-ground channels [17]. Thus, we have

$$\frac{C^2 \mathrm{Var}\{\tilde{\rho}_{i,k}^{t_0}(t)\}}{(2\ln 2)(1 + \mathbb{E}\{\tilde{\rho}_{i,k}^{t_0}(t)\} C\left(d_k(R,t)\right)^{-2})^2} - o < \frac{\mathrm{Var}\{\tilde{\rho}_{i,k}^{t_0}(t)\}}{(2\ln 2)(\mathbb{E}\{\tilde{\rho}_{i,k}^{t_0}(t)\})^2} \approx 0. \tag{10}$$

In this case, we can obtain

$$H_{i,k}\left(t, \tilde{\rho}_{i,k}^{t_0}(t)\right) \approx s_{i,k}(t) T_s B \log_2\left(1 + \mathbb{E}\left\{\tilde{\rho}_{i,k}^{t_0}(t)\right\} C\left(d_k(R,t)\right)^{-2}\right). \tag{11}$$

In this section, we give the formulation for TPRA problem under perfect prediction of channel coefficients. However, this formulation is overwhelmingly idealistic for practical applications. In Section 4, we give the robust TPRA algorithm considering prediction errors of channel coefficients.

4 Robust TPRA under prediction error

In this section, we study the robust TPRA algorithm, which considers the prediction errors of channel coefficients. We first formulate a robust optimization problem with chance constraints, where the deterministic equivalent forms of chance constraints are obtained by a tractable approximation. Then, we solve the optimization problem with a modified SCA method. Finally, to cater to the high-mobility features of UAV communication networks, a low-complexity algorithm is proposed to obtain real-time TPRA.

4.1 Tractable approximation for chance constraint

In problem (P1), the expected data received by GUs is directly evaluated according to the predicted channel coefficients, which ignores the prediction error of channel coefficients. However, the prediction error has significant impact on the QoS of GUs. Let $\psi_{i,k}^{t_0}(t)$ denote the prediction error of $\mathbb{E}\{\tilde{\rho}_{i,k}^{t_0}(t)\}$, whose variance is defined as $\sigma_{i,k}^{t_0}(t)$. In addition, let $\Psi_{t_0} = \{\psi_{1,1}^{t_0}(1), \ldots, \psi_{N_F,K}^{t_0}(N_T)\}$. Defining $\tilde{H}_{i,k}(t, \tilde{\rho}_{i,k}^{t_0}(t), \psi_{i,k}^{t_0}(t))$ as the predicted channel transmission rate under prediction error, we have

$$\tilde{H}_{i,k}\left(t, \tilde{\rho}_{i,k}^{t_0}(t), \psi_{i,k}^{t_0}(t)\right) = s_{i,k}(t) T_s B \log_2\left(1 + \left(\mathbb{E}\left\{\tilde{\rho}_{i,k}^{t_0}(t)\right\} + \psi_{i,k}^{t_0}(t)\right) C\left(d_k(R,t)\right)^{-2}\right). \tag{12}$$

We rewrite the QoS constraint C1a as a chance constraint form:

$$\text{C1b}: \ \Pr\left\{A_{k,t_0} + \sum_{t\in\mathcal{T}_{t_0}}\sum_{i\in\mathcal{I}}\tilde{H}_{i,k}\left(t, \tilde{\rho}_{i,k}^{t_0}(t), \psi_{i,k}^{t_0}(t)\right) \geqslant N_Q S K\right\} \geqslant 1 - \varepsilon, \quad \forall k \in \mathcal{K}. \tag{13}$$

Note that the QoS constraints of GUs are satisfied with a predefined probability. Specifically, $0 < \varepsilon \ll 1$ is the maximum probability that the QoS of GUs cannot be satisfied. Constraint C1b is a chance constraint, which is in general computationally intractable. In this case, a natural process is to replace constraint C1b with a safe tractable approximation defined on a space contained in the feasible set of the initial constraint. Accordingly, the feasible solution to the safe tractable approximation is feasible for the original chance constraint.

To obtain a deterministic equivalent form of the chance constraint by a tractable approximation, the chance constraint generally is represented as a linear summation of random variables [22]. Hence, we first linearize constraint C1b. We define an auxiliary function as

$$J\left(k, \tilde{\boldsymbol{\rho}}_{t_0}, \Psi_{t_0}\right) = N_Q S K - A_{k,t_0} - \sum_{t\in\mathcal{T}_{t_0}}\sum_{i\in\mathcal{I}}\tilde{H}_{i,k}\left(t, \tilde{\rho}_{i,k}^{t_0}(t), \psi_{i,k}^{t_0}(t)\right). \tag{14}$$

We first fix R and $\boldsymbol{s}$, and consider constraint C1b that dependes on Ψ_{t_0}. We perform a linearization of $J\left(k, \tilde{\boldsymbol{\rho}}_{t_0}, \Psi_{t_0}\right)$ with respect to Ψ_{t_0} and consider the approximation [23, 24]:

$$J\left(k, \tilde{\boldsymbol{\rho}}_{t_0}, \Psi_{t_0}\right) \approx J\left(k, \tilde{\boldsymbol{\rho}}_{t_0}, \mathbf{0}\right) + \sum_{t\in\mathcal{T}_{t_0}}\sum_{i\in\mathcal{I}}\frac{\partial J\left(k, \tilde{\boldsymbol{\rho}}_{t_0}, \Psi_{t_0}\right)}{\partial\psi_{i,k}^{t_0}(t)}\bigg|_{\Psi_{t_0}=\mathbf{0}}\psi_{i,k}^{t_0}(t) \tag{15}$$

for $\psi_{i,k}^{t_0}(t) \in [-3\sigma_{i,k}^{t_0}(t), +3\sigma_{i,k}^{t_0}(t)], \forall i \in \mathcal{I}, k \in \mathcal{K}, t \in \mathcal{T}_{t_0}$. This approximation is valid with small $\sigma_{i,k}^{t_0}(t)$, which is satisfied in the UAV system [17, 23]. Furthermore, in (15), we have

$$\frac{\partial J\left(k, \tilde{\boldsymbol{\rho}}_{t_0}, \Psi_{t_0}\right)}{\partial\psi_{i,k}^{t_0}(t)}\bigg|_{\Psi_{t_0}=\mathbf{0}} = \frac{-s_{i,k}(t) T_s B C\left(d_k(R,t)\right)^{-2}}{(\ln 2)\left(1 + \mathbb{E}\{\tilde{\rho}_{i,k}^{t_0}(t)\}C\left(d_k(R,t)\right)^{-2}\right)}. \tag{16}$$

For simplicity of notation, in the following, we replace $\frac{\partial J(k,\tilde{\boldsymbol{\rho}}_{t_0},\Psi_{t_0})}{\partial\psi_{i,k}^{t_0}(t)}|_{\Psi_{t_0}=\mathbf{0}}$ with $J'(i,k,t,\tilde{\boldsymbol{\rho}}_{t_0})$. Substituting (15) into constraint C1b, we can obtain

$$\Pr\left\{J\left(k, \tilde{\boldsymbol{\rho}}_{t_0}, \mathbf{0}\right) + \sum_{t\in\mathcal{T}_{t_0}}\sum_{i\in\mathcal{I}}J'\left(i,k,t,\tilde{\boldsymbol{\rho}}_{t_0}\right)\psi_{i,k}^{t_0}(t) \leqslant 0\right\} \geqslant 1 - \varepsilon, \tag{17}$$

which is a linear summation of random variables $\psi_{i,k}^{t_0}(t), \forall i \in \mathcal{I}, t \in \mathcal{T}_{t_0}, k \in \mathcal{K}$. Hence, constraint (17) can be rewritten as an equivalent constraint [22]:

$$\text{C1c}: \ J\left(k, \tilde{\boldsymbol{\rho}}_{t_0}, \mathbf{0}\right) + \text{ErfInv}\left(\varepsilon\right)\sqrt{\sum_{t\in\mathcal{T}_{t_0}}\sum_{i\in\mathcal{I}}\left(\sigma_{i,k}^{t_0}(t) J'\left(i,k,t,\tilde{\boldsymbol{\rho}}_{t_0}\right)\right)^2} \leqslant 0, \tag{18}$$

where $\mathrm{ErfInv}(\varepsilon)$ is the inverse error function satisfying

$$\frac{1}{\sqrt{2\pi}} \int_{\mathrm{ErfInv}(v)}^{\infty} \exp\left\{-r^2/2\right\} \mathrm{d}r = v, \quad 0 < v < 1.$$

As we can see, the equivalent constraint (18) is independent on the random variables $\psi_{i,k}^{t_0}(t), \forall i \in \mathcal{I}, k \in \mathcal{K}, t \in \mathcal{T}_{t_0}$, thereby being a deterministic form constraint. Accordingly, problem (P2) can be rewritten as

$$(\mathrm{P2}') \quad \max_{R,\boldsymbol{s}} \frac{1}{E(R)} \left(\sum_{k \in \mathcal{K}} A_{k,t_0} + \sum_{t \in \mathcal{T}_{t_0}} \sum_{i \in \mathcal{I}} \sum_{k \in \mathcal{K}} \tilde{H}_{i,k}\left(t, \tilde{\rho}_{i,k}^{t_0}(t), 0\right) \right)$$
$$\text{s.t. } \mathrm{C1c}, \ \mathrm{C2} - \mathrm{C5}.$$

Remark 1. Note that constraint C1c is a second-order cone constraint with respect to $\boldsymbol{s}$ for a given hover radius R.

4.2 Optimal solution of TPRA

In the considered UAV communication network, the UAV will hover over the target area with a fixed radius R. Thus, the hover radius should be optimized once at the beginning of the flight cycle. During the flight cycle, the UAV only optimizes the subcarrier allocation strategy according to the real-time predicted channel coefficients. At the end of flight cycle, the UAV can improve the prediction algorithm to reduce the prediction error of channel coefficients, and further obtain a more appropriate hover radius at the beginning of the next flight cycle. In the following, the programming processed at the beginning of each flight cycle is called the hover radius and resource allocation (HRRA) programming, and the program during the flight cycle is called the resource allocation (RA) programming.

4.2.1 *HRRA programming*

At the beginning of the flight cycle, the hover radius and resource allocation strategy are both optimized. In this case, we have $t_0 = 0$ and $\sum_{k \in \mathcal{K}} A_{k,0} = 0$. Hence, problem (P2′) can be written as

$$(\mathrm{P3}) \quad \max_{R,\boldsymbol{s}} \frac{1}{E(R)} \left(\sum_{t \in \mathcal{T}_0} \sum_{i \in \mathcal{I}} \sum_{k \in \mathcal{K}} \tilde{H}_{i,k}\left(t, \tilde{\rho}_{i,k}^{0}(t), 0\right) \right)$$
$$\text{s.t. } \mathrm{C1c}, \ \mathrm{C2} - \mathrm{C5}.$$

As we can see, the objective function of problem (P3) is a single ratio fractional function. Thus, we first use Dinkelbach's Transform to reformulate problem (P3) as

$$(\mathrm{P3}') \quad \min_{R,\boldsymbol{s}} yE(R) - G(R, \boldsymbol{s}, \tilde{\boldsymbol{\rho}}_0)$$
$$\text{s.t. } \mathrm{C1c}, \ \mathrm{C2} - \mathrm{C5},$$

where $G(R, \boldsymbol{s}, \tilde{\boldsymbol{\rho}}_0)$ is given by

$$G(R, \boldsymbol{s}, \tilde{\boldsymbol{\rho}}_0) = \sum_{t \in \mathcal{T}_0} \sum_{i \in \mathcal{I}} \sum_{k \in \mathcal{K}} \tilde{H}_{i,k}\left(t, \tilde{\rho}_{i,k}^{0}(t), 0\right). \tag{19}$$

In addition, y is an auxiliary variable. Specifically, y is iteratively updated by

$$y^{(m+1)} = \frac{G\left(R^{(m)}, \boldsymbol{s}^{(m)}, \tilde{\boldsymbol{\rho}}_0\right)}{E\left(R^{(m)}\right)}, \tag{20}$$

where m is the outer iteration index. $R^{(m)}$ and $\boldsymbol{s}^{(m)}$ are the optimal solution of the m-th iteration. It can be proved that convergence is guaranteed by alternatively updating y according to (20) since y is non decreasing after each iteration [25]. In problem (P3′), the objective function is not a concave function, and constraint C1c is not a convex constraint. Define auxiliary variate $x_{i,k}(t)$ with $x_{i,k}(t) \leqslant \frac{s_{i,k}(t)}{(d_k(R,t))^2}$. Let

$\boldsymbol{d} = \{d_k(t), \forall k \in \mathcal{K}, t \in \mathcal{T}_0\}$ and $\boldsymbol{x} = \{\boldsymbol{x}_k, \forall k \in \mathcal{K}\}$ with $\boldsymbol{x}_k = \{x_{i,k}(t), \forall i \in \mathcal{I}, t \in \mathcal{T}_0\}$. With auxiliary variate $x_{i,k}(t)$, we can rewrite (12) as

$$
\begin{aligned}
\tilde{H}_{i,k}\left(t, \tilde{\rho}_{i,k}^{t_0}(t), \psi_{i,k}^{t_0}(t)\right) &= T_{\mathrm{s}}B\log_2\left(1 + \left(\mathbb{E}\left\{\tilde{\rho}_{i,k}^{t_0}(t)\right\} + \psi_{i,k}^{t_0}(t)\right)C\frac{s_{i,k}(t)}{(d_k(R,t))^2}\right) \\
&\geqslant T_{\mathrm{s}}B\log_2\left(1 + \left(\mathbb{E}\left\{\tilde{\rho}_{i,k}^{t_0}(t)\right\} + \psi_{i,k}^{t_0}(t)\right)Cx_{i,k}(t)\right).
\end{aligned}
\tag{21}
$$

Similarly, Eq. (16) can be rewritten as

$$
\begin{aligned}
\left.\frac{\partial J\left(k, \tilde{\boldsymbol{\rho}}_{t_0}, \Psi_{t_0}\right)}{\partial \psi_{i,k}^{t_0}(t)}\right|_{\Psi_{t_0}=\boldsymbol{0}} &= \frac{-s_{i,k}(t)T_{\mathrm{s}}BC\left(d_k(R,t)\right)^{-2}}{(\ln 2)\left(1 + s_{i,k}(t)\mathbb{E}\{\tilde{\rho}_{i,k}^{t_0}(t)\}C\left(d_k(R,t)\right)^{-2}\right)} \\
&\geqslant \frac{-T_{\mathrm{s}}BCx_{i,k}(t)}{(\ln 2)\left(1 + \mathbb{E}\{\tilde{\rho}_{i,k}^{t_0}(t)\}Cx_{i,k}(t)\right)}.
\end{aligned}
\tag{22}
$$

Accordingly, problem (P3′) can be written as

$$
\begin{aligned}
(\text{P4}) \quad &\min_{R, \boldsymbol{s}, \boldsymbol{x}, \boldsymbol{d}} \; yE(R) - G_1(\boldsymbol{x}) \\
&\text{s.t. } \text{C2} - \text{C6}, \\
&\quad \text{C1d}: \; U(k, \tilde{\boldsymbol{\rho}}_0, \boldsymbol{x}) + N_{\mathrm{Q}}SK \leqslant 0, \; \forall k \in \mathcal{K}, \\
&\quad \text{C7}: \; 0 \leqslant x_{i,k}(t) \leqslant \frac{s_{i,k}(t)}{(d_k(R,t))^2}, \; \forall i \in \mathcal{I}, \; k \in \mathcal{K}, \; t \in \mathcal{T}_0,
\end{aligned}
$$

where $G_1(\boldsymbol{x}) = \sum_{t\in\mathcal{T}_0}\sum_{i\in\mathcal{I}}\sum_{k\in\mathcal{K}} T_{\mathrm{s}}B\log_2(1+\mathbb{E}\{\tilde{\rho}_{i,k}^0(t)\}Cx_{i,k}(t))$. Moreover, in problem (P4), $U(k, \tilde{\boldsymbol{\rho}}_0, \boldsymbol{x})$ is given by

$$
\begin{aligned}
U(k, \tilde{\boldsymbol{\rho}}_0, \boldsymbol{x}) = &-\sum_{t\in\mathcal{T}_0}\sum_{i\in\mathcal{I}} T_{\mathrm{s}}B\log_2\left(1 + \mathbb{E}\left\{\tilde{\rho}_{i,k}^0(t)\right\}Cx_{i,k}(t)\right) \\
&+ \mathrm{ErfInv}(\varepsilon)\sqrt{\sum_{t\in\mathcal{T}_0}\sum_{i\in\mathcal{I}}\left(\frac{\sigma_{i,k}^0(t)T_{\mathrm{s}}BCx_{i,k}(t)}{(\ln 2)\left(1 + \mathbb{E}\{\tilde{\rho}_{i,k}^0(t)\}Cx_{i,k}(t)\right)}\right)^2}.
\end{aligned}
\tag{23}
$$

Lemma 1. $\sqrt{\sum_{t\in\mathcal{T}_0}\sum_{i\in\mathcal{I}}\left(\frac{\sigma_{i,k}^0(t)T_{\mathrm{s}}BCx_{i,k}(t)}{(\ln 2)(1+\mathbb{E}\{\tilde{\rho}_{i,k}^0(t)\}Cx_{i,k}(t))}\right)^2}$ is a quasiconvex function with respect to $\boldsymbol{x}_k$.

Proof. Please refer to Appendix.

Aided by Lemma 1, we can obtain the following theorem.

Theorem 1. Constraint C1d is a convex constraint.

Proof. Please refer to Appendix.

In problem (P4), the objective function and constraint C1d are convex function and convex constraint, respectively. However, in problem (P4), constraints C4 and C7 are still not convex constraints. For constraint C4, we relax integer constraints on variables $s_{i,k}(t)$ as $s_{i,k}(t) \in [0,1]$. In addition, we apply constraint $s_{i,k}(t) = s_{i,k}^2(t)$ to ensure that $s_{i,k}(t)$ is a binary variable. This constraint is equivalent to the set of condition $\{s_{i,k}(t) \leqslant s_{i,k}^2(t), s_{i,k}(t) \geqslant s_{i,k}^2(t)\}$. It can be obtained that $s_{i,k}(t) \geqslant s_{i,k}^2(t)$ always holds due to $s_{i,k}(t) \in [0,1]$. Thus, we can replace constrain C4 with the following two constraints:

$$
\text{C4a}: \; s_{i,k}(t) \in [0,1], \; \forall i \in \mathcal{I}, \; t \in \mathcal{T}, \; k \in \mathcal{K},
\tag{24}
$$

$$
\text{C4b}: \; \sum_{t\in\mathcal{T}_0}\sum_{i\in\mathcal{I}}\sum_{k\in\mathcal{K}}\left(s_{i,k}(t) - s_{i,k}^2(t)\right) \leqslant 0.
\tag{25}
$$

Moreover, constraint C7 can be written as

$$
\text{C7a}: \; -\log\left(s_{i,k}(t) + \rho\right) + \log\left(x_{i,k}(t) + \rho\right) + 2\log\left(d_k(R,t)\right) \leqslant 0, \; \forall i \in \mathcal{I}, \; k \in \mathcal{K}, \; t \in \mathcal{T}_0,
\tag{26}
$$

$$
\text{C7b}: \; x_{i,k}(t) \geqslant 0, \; \forall i \in \mathcal{I}, \; k \in \mathcal{K}, \; t \in \mathcal{T}_0,
\tag{27}
$$

where $0 < \rho \ll 1$ is a constant ensuring $s_{i,k}(t) + \rho > 0$. Since constraints C4b and C7a are not convex, we use SCA method to solve the problem (P4). For SCA method, variables are updated successively until converging to the minimum of the approximated version of the objective function, which is a tight lower bound of the objective function. Particularly, let $F(s_{i,k}(t)) = s_{i,k}(t) - s_{i,k}^2(t)$. For any given point $s_{i,k}^{(m)}(t)$, we have

$$F(s_{i,k}(t)) \geqslant s_{i,k}^{(m)}(t) - \left(s_{i,k}^{(m)}(t)\right)^2 + \left(1 - 2s_{i,k}^{(m)}(t)\right)\left(s_{i,k}(t) - s_{i,k}^{(m)}(t)\right)$$
$$\triangleq \underline{F}(s_{i,k}(t)). \tag{28}$$

Let $Q(s_{i,k}(t), x_{i,k}(t), d_k(R,t)) = -\log(s_{i,k}(t) + \rho) + (\log(x_{i,k}(t) + \rho) + 2\log(d_k(R,t)))$. For given $s_{i,k}^{(m)}(t), x_{i,k}^{(m)}(t)$, and $d_k^{(m)}(R,t)$, we have

$$\begin{aligned}
&Q(s_{i,k}(t), x_{i,k}(t), d_k(R,t)) \\
&\geqslant -\log\left(s_{i,k}^{(m)}(t) + \rho\right) + \log\left(x_{i,k}^{(m)}(t) + \rho\right) + 2\log\left(d_k^{(m)}(R,t)\right) \\
&\quad + \left(-\frac{1}{s_{i,k}^{(m)}(t) + \rho} + \frac{1}{x_{i,k}^{(m)}(t) + \rho} + \frac{2}{d_k^{(m)}(R,t)}\right) \\
&\quad \times \left(s_{i,k}(t) - s_{i,k}^{(m)}(t) + x_{i,k}(t) - x_{i,k}^{(m)}(t) + d_k(R,t) - d_k^{(m)}(R,t)\right) \\
&\triangleq \underline{Q}(s_{i,k}(t), x_{i,k}(t), d_k(R,t)). \tag{29}
\end{aligned}$$

Then, we can find a lower bound of problem (P4) by solving the following optimization program:

$$(\text{P4}') \quad \min_{R, \boldsymbol{x}, \boldsymbol{s}, \boldsymbol{d}} yE(R) - G_1(\boldsymbol{x}) - \xi_1 \sum_{t \in \mathcal{T}_0} \sum_{i \in \mathcal{I}} \sum_{k \in \mathcal{K}} \underline{F}(s_{i,k}(t)) - \sum_{t \in \mathcal{T}_0} \sum_{i \in \mathcal{I}} \sum_{k \in \mathcal{K}} \mu_{i,k}(t) \underline{Q}(s_{i,k}(t), x_{i,k}(t), d_k(R,t))$$
$$\text{s.t. C1d, C2, C3, C4a, C5, C6, C7b.}$$

Note that problem (P4$'$) is convex and can be solved by standard optimization problem method, such as internal point method. We can iteratively tighten the obtained lower bound. Let $\Xi^{(m)} = \{R^{(m)}, \boldsymbol{x}^{(m)}, \boldsymbol{s}^{(m)}, \boldsymbol{d}^{(m)}\}$ denote the solution of m-th iteration and give a tolerance level $\varepsilon_1 > 0$. The iteration process will be stopped if $\frac{|\Xi^{(m)} - \Xi^{(m-1)}|}{|\Xi^{(m-1)}|} \leqslant \varepsilon_1$. The algorithm is summarized in Algorithm 1.

Algorithm 1 Successive convex approximation

1: **Initialization**
2: Initialize iteration index $m = 1$ and initial point $\Xi^{(0)}$.
3: Set tolerance level $\varepsilon_1 \ll 1$.
4: **repeat**
5:     For given $\Xi^{(m-1)}$, solve problem (P4$'$), and obtain solution $\Xi^{(m)}$.
6:     Set $m = m + 1$.
7: **until** $\frac{|\Xi^{(m)} - \Xi^{(m-1)}|}{|\Xi^{(m-1)}|} \leqslant \varepsilon_1$.
8: Adjust resource allocation strategy $\boldsymbol{s}$ following rule (32) to obtain $\boldsymbol{s}^*$.
9: Solve problem (P4$''$) and obtain the optimal solution Ξ^*.

Suppose $\bar{\Xi} = \{\bar{R}, \bar{\boldsymbol{x}}, \bar{\boldsymbol{s}}, \bar{\Theta}\}$ is the solution found by Algorithm 1. It should be noted that there is still no guarantee that $\bar{\Xi}$ is the optimal solution of problem (P4) [26]. Particularly, $\bar{\boldsymbol{s}}$ may be still not binary but only nearly binary. Therefore, we adjust $\bar{\boldsymbol{s}}$ by following the rule as below:

$$s_{i,k}^*(t) = \begin{cases} 1, & \text{if } \bar{s}_{i,k}(t) > 0.5, \\ 0, & \text{if } \bar{s}_{i,k}(t) \leqslant 0.5. \end{cases} \tag{30}$$

Final, we improve the solution of problem (P4) by solving the following convex program with given $\boldsymbol{s}^*$:

$$(\text{P4}'') \quad \min_{R, \boldsymbol{x}, \boldsymbol{d}} yE(R) - G_1(\boldsymbol{x})$$
$$\text{s.t. C1d, C5, C7.}$$

The total algorithm is summarized in Algorithm 1. Let $\{R^*, \boldsymbol{x}^*, \boldsymbol{d}^*\}$ denote the solution of problem (P4$''$). It has been proved that $\Xi^* = \{R^*, \boldsymbol{x}^*, \boldsymbol{s}^*, \boldsymbol{d}^*\}$ is the optimal solution of problem (P4) [26]. The total algorithm is summarized in Algorithm 2.

Algorithm 2 The HRRA programming

1: **Initialization**
2: Initialize iteration index $m = 1$ and initial y.
3: Set tolerance level $\varepsilon_2 \ll 1$.
4: **repeat**
5:     For given $y^{(m)}$, solve problem (P4), and obtain the optimal solution Ξ^*.
6:     Calculate $G(R, \boldsymbol{s}, \boldsymbol{h}_0)$ and $E(R)$.
7:     Set $m = m + 1$ and calculate $y^{(m+1)}$ according to (20).
8: **until** $\frac{|y^{(m)} - y^{(m-1)}|}{|y^{(m-1)}|} \leqslant \varepsilon_2$.

4.2.2 *RA programming*

Since the hover radius is constant during the flight cycle, we only need to optimize the resource allocation strategy based on the real-time predicted channel coefficients.

Let R^* denote the optimal hover radius found by Algorithm 2. In this case, problem (P2′) can be written as

$$(P6) \quad \max_{\boldsymbol{s}} \sum_{k \in \mathcal{K}} A_{k,t_0} + \sum_{t \in \mathcal{T}_{t_0}} \sum_{i \in \mathcal{I}} \sum_{k \in \mathcal{K}} \tilde{H}_{i,k}\left(t, \tilde{\rho}_{i,k}^0\left(t\right), 0\right)$$

$$\text{s.t. } C1c, C2 - C4,$$

where t_0 is the index of current time slot. According to Remark 1, constraint C1c is a second-order cone constraint with respect to $\boldsymbol{s}$. Thus, problem (P6) is a convex 0-1 integer programming, which can be optimally solved by SCA method mentioned in Algorithm 1.

4.3 Low-complexity online algorithm

In this subsection, we will give the low-complexity online algorithm for real-time TPRA. Generally, the UAV-mounted processor cannot provide high computing capability. Hence, the proposed TPRA algorithm should be completed in the shortest possible time. We take the HRRA programming as an example to illustrate the low-complexity algorithm.

Initialization. To begin with, we give the initial hover radius $R^{(0)}$, which is obtained by minimizing $E(R)$, i.e., $R^{(0)} = \arg\min_R E(R)$. Note that the initial hover radius $R^{(0)}$ is the smallest energy consumption radius. Then, we obtain the initial subcarrier allocation policy $\boldsymbol{s}^{(0)}$ with the following rule:

$$s_{i,k}^0\left(t\right) = \begin{cases} 1, & \text{if } i = \arg\max_j \tilde{\rho}_{i,k}^0\left(t\right), \\ 0, & \text{otherwise.} \end{cases} \tag{31}$$

According to $\boldsymbol{s}^{(0)}$, the amount of received data for each GU during one flight cycle can be evaluated by the robust rule shown in Subsection 4.1.

$$r_k\left(\boldsymbol{s}, \tilde{\boldsymbol{\rho}}_0, R\right) = \sum_{t \in \mathcal{T}_0} \sum_{i \in \mathcal{I}} T_{\mathrm{s}} B \log_2 \left(1 + \mathbb{E}\left\{\tilde{\rho}_{i,k}^0\left(t\right)\right\} C \frac{s_{i,k}\left(t\right)}{\left(d_k\left(R,t\right)\right)^2}\right)$$

$$- \mathrm{ErfInv}\left(\varepsilon\right) \sqrt{\sum_{t \in \mathcal{T}_0} \sum_{i \in \mathcal{I}} \left(\frac{\sigma_{i,k}^0\left(t\right) T_{\mathrm{s}} B C \frac{s_{i,k}(t)}{\left(d_k(R,t)\right)^2}}{\left(\ln 2\right)\left(1 + \mathbb{E}\{\tilde{\rho}_{i,k}^0\left(t\right)\} C \frac{s_{i,k}(t)}{\left(d_k(R,t)\right)^2}\right)}\right)^2}. \tag{32}$$

If $r_k\left(\boldsymbol{s}, \tilde{\boldsymbol{\rho}}_0, R\right) \geqslant N_{\mathrm{Q}} S K, \forall k \in \mathcal{K}$, the initial subcarrier allocation policy $\boldsymbol{s}^{(0)}$ is the best one. Otherwise, we define the lower bound of QoS, and alternately tighten the lower bound to satisfy the QoS constraints of GUs. Specifically, we define the initial lower bound of QoS as follows:

$$\underline{w}^{(0)} = \min_{k \in \mathcal{K}} \left\{ \sum_{t \in \mathcal{T}_0} \sum_{i \in \mathcal{I}} \tilde{H}_{i,k}\left(t, \tilde{\rho}_{i,k}^0\left(t\right), 0\right), N_{\mathrm{Q}} S K \right\}. \tag{33}$$

Furthermore, the amount of transmitted data for GU k occupying subcarrier i at time slot t can be given by

$$\bar{r}_k\left(i, t\right) = T_{\mathrm{s}} B \log_2 \left(1 + \frac{\mathbb{E}\{\tilde{\rho}_{i,k}^0\left(t\right)\} C}{\left(d_k\left(R,t\right)\right)^2}\right). \tag{34}$$

Iteration. Consider the n-th iteration for optimizing subcarrier allocation policy. Let $\underline{w}^{(n-1)}$ and $R^{(n-1)}$ denote the lower bound of QoS and hover radius in the $(n-1)$-th iteration, respectively. Moreover, let $r_k^{(n-1)}$ denote the amount of received data based on $R^{(n-1)}$ and $\boldsymbol{s}^{(n-1)}$. Let $\mathcal{S}_{\mathrm{Y}}$ and $\mathcal{S}_{\mathrm{N}}$ denote the sets of GUs satisfying the lower bound of QoS constraint, i.e., $r_k^{(n-1)} \geqslant \underline{w}^{(n-1)}$, and not, respectively. Then, for GU $k = \arg\min_{k_1 \in \mathcal{S}_{\mathrm{N}}} r_{k_1}^{(n-1)}$, set the tuple (i', t', k') as

$$(i', t', k') = \underset{i \in \mathcal{I}, t \in \mathcal{T}_0, k_1 \in \mathcal{K}_1}{\arg\max} \frac{\bar{r}_{k_1}(i, t)\, s_{i,k_1}^{(n-1)}(t)\, / r_{k_1}^{(n-1)}}{\bar{r}_k(i, t)\, / r_k^{(n-1)}}, \tag{35}$$

where $\mathcal{K}_1 = \mathcal{S}_{\mathrm{Y}} \setminus \{k\}$. If $r_{k'}^{(n-1)} - \bar{r}_{k'}(i', t') \geqslant \underline{w}^{(n-1)}$, we set $s_{i',k'}^{(n)}(t') = 0$ and $s_{i',k}^{(n)}(t') = 1$. Otherwise, setting $\mathcal{K}_1 = \mathcal{K}_1 \setminus \{k'\}$, choose repeatedly (i', t', k') until $\mathcal{K}_1 = \emptyset$. After obtaining $\boldsymbol{s}^{(n)}$, update lower bound of QoS constraint $\underline{w}^{(n)}$ according to (33). If $\underline{w}^{(n)} \geqslant N_{\mathrm{Q}}SK$, the subcarrier allocation policy $\boldsymbol{s}^{(n)}$ is the best one. Otherwise, repeat above processing until $\underline{w}^{(n)} - \underline{w}^{(n-1)} \leqslant \varepsilon_4$.

If $\underline{w}^{(n)} < N_{\mathrm{Q}}SK$, we need to update the hover radius R as follows. Consider the m-th iteration for optimizing hove radius. Let $\mathcal{K}_{\mathrm{in}}$ denote the set of GUs whose distance to the hover center is smaller than $R^{(m-1)}$. Similarly, $\mathcal{K}_{\mathrm{out}}$ denotes the set of GUs whose distance to the hover center is larger than $R^{(m-1)}$. Then, we define

$$\mathrm{QoS}_{\mathrm{in}} = \sum_{k \in \mathcal{K}_{\mathrm{in}}} \min \left\{ \sum_{t \in \mathcal{T}_0} \sum_{i \in \mathcal{I}} \tilde{H}_{i,k}\left(t, \tilde{\rho}_{i,k}^0(t), 0\right) - N_{\mathrm{Q}}SK, 0 \right\}, \tag{36}$$

and

$$\mathrm{QoS}_{\mathrm{out}} = \sum_{k \in \mathcal{K}_{\mathrm{out}}} \min \left\{ \sum_{t \in \mathcal{T}_0} \sum_{i \in \mathcal{I}} \tilde{H}_{i,k}\left(t, \tilde{\rho}_{i,k}^0(t), 0\right) - N_{\mathrm{Q}}SK, 0 \right\}. \tag{37}$$

In each iteration, the hover radius is updated by

$$R^{(m)} = R^{(m-1)} + \triangle R^{(m)} \frac{QoS_{\mathrm{in}} - QoS_{\mathrm{out}}}{|QoS_{\mathrm{in}}| + |QoS_{\mathrm{out}}|}. \tag{38}$$

In (38), we have $\triangle R^{(m)} = \max\left\{\triangle R_{\min}, \theta \triangle R^{(m-1)}\right\}$, where $\triangle R_{\min}$ is the minimum value of hover radius adjustment and $0 < \theta < 1$. After updating hover radius R, we repeatedly optimize the subcarrier allocation policy. Note that lower bound of QoS is non-decreasing after each iteration. Thus, lower bound of QoS will tend to be $N_{\mathrm{Q}}SK$ as the number of iterations increases.

Stopping criterion. The iteration will stop until

$$\frac{\left| U\left(R^{(m)}, \boldsymbol{s}^{(m)}, \tilde{\boldsymbol{\rho}}_0\right) - U\left(R^{(m-1)}, \boldsymbol{s}^{(m-1)}, \tilde{\boldsymbol{\rho}}_0\right) \right|}{\left| U\left(R^{(m-1)}, \boldsymbol{s}^{(m-1)}, \tilde{\boldsymbol{\rho}}_0\right) \right|} \leqslant \varepsilon_3, \tag{39}$$

where ε_3 is the error tolerance for Algorithm 3 and

$$U\left(R^{(m)}, \boldsymbol{s}^{(m)}, \tilde{\boldsymbol{\rho}}_0\right) = G\left(R^{(m)}, \boldsymbol{s}^{(m)}, \tilde{\boldsymbol{\rho}}_0\right) - y E\left(R^{(m)}\right). \tag{40}$$

The proposed low-complexity algorithm summarized in Algorithm 3. The RA programming can also be solved by the similar algorithm shown in Algorithm 3.

Complexity analysis. We analyze the computational complexity of the proposed low-complexity algorithm and compare it against the optimal. Problem (P4′) is a SoCP programming, which can be solved by interior point method. The worst case of interior point method requires $\mathcal{O}\left(\sqrt{N_{\mathrm{Con}}}\right)$ iterations, where N_{Con} is the number of constraints. Moreover, each iteration has a complexity of $\mathcal{O}(m^2 \sum_{i=1}^{N_{\mathrm{Con}}} n_i)$, where m is the number of variables, and n_i is the dimension of the i-th constraint. Therefore, the complexity of the optimal algorithm is

$$\mathcal{O}\left(l\sqrt{K + 2N_TK + N_{\mathrm{F}}N_T + 3N_{\mathrm{F}}N_TK}\, (N_{\mathrm{F}}N_TK)^2\, (2K + 2N_TK + N_{\mathrm{F}}N_T + 3N_{\mathrm{F}}N_TK)\right)$$

$$\approx \mathcal{O}\left(l\, (N_{\mathrm{F}}N_TK)^2\, (2N_TK + N_{\mathrm{F}}N_T + 3N_{\mathrm{F}}N_TK)^{3/2}\right),$$

Algorithm 3 The low-complexity algorithm

1: **Initialization**
2: Initialize iteration index $m = 1$, and set tolerance level $\varepsilon_3 \ll 1$.
3: Give $R^{(0)}$, $\boldsymbol{s}^{(0)}$.
4: **repeat**
5:     Set $n = 1$.
6:     **repeat**
7:         Obtain $\underline{w}^{(n-1)}$, $R^{(n-1)}$, $r_k^{(n-1)}$, $\mathcal{S}_{\mathrm{Y}}$ and $\mathcal{S}_{\mathrm{N}}$.
8:         Set $k = \arg\min_{k_1 \in \mathcal{S}_{\mathrm{N}}} r_{k_1}^{(n-1)}$ and $\mathcal{K}_1 = \mathcal{S}_{\mathrm{Y}} \setminus \{k\}$.
9:         **repeat**
10:             Obtain the tuple (i', t', k') according to (35).
11:             **if** $r_{k'}^{(n-1)} - \bar{r}_{k'}(i', t') \geqslant \underline{w}^{(n-1)}$,
12:                 set $s_{i',k'}^{(n)}(t') = 0$ and $s_{i',k}^{(n)}(t') = 1$.
13:                 Break.
14:             **else**
15:                 Set $\mathcal{K}_1 = \mathcal{K}_1 \setminus \{k'\}$.
16:             **end**
17:         **until** $\mathcal{K}_1 = \emptyset$
18:         **if** $\mathcal{K}_1 == \emptyset$ or $\underline{w}^{(n)} \geqslant N_{\mathrm{Q}} SK$,
19:             Break.
20:         **end**
21:         Set $n = n + 1$.
22:     **until** $n ==$ Loop or $\underline{w}^{(n)} - \underline{w}^{(n-1)} \leqslant \varepsilon_4$.
23:     **if** $\underline{w}^{(n)} \geqslant N_{\mathrm{Q}} SK$,
24:         Break.
25:     **end**
26:     Update hover radius according to (36).
27:     Set $m = m + 1$.
28: **until** $\frac{|U(R^{(m)}, \boldsymbol{s}^{(m)}, \tilde{\rho}_0) - U(R^{(m-1)}, \boldsymbol{s}^{(m-1)}, \tilde{\rho}_0)|}{|U(R^{(m-1)}, \boldsymbol{s}^{(m-1)}, \tilde{\rho}_0)|} \leqslant \varepsilon_3$ or $m ==$ Loop.
29: **return** The final resource allocation strategy and hover radius.

---

where l is the number of SCA iterations. For the proposed low-complexity algorithm in Algorithm 3, the computation of $w^{(n)}$ and $r_k^{(n)}$ has a complexity of $\mathcal{O}(N_{\mathrm{F}} N_T K)$. Each adjustment of subcarrier allocation policy has a complexity of $\mathcal{O}(N_{\mathrm{F}} N_T)$. Hence, the total complexity of the low-complexity algorithm is $\mathcal{O}(l_2 l_3 (N_{\mathrm{F}} N_T K + N_{\mathrm{F}} N_T))$, where l_2 and l_3 are the number of inner iterations and outer iterations, respectively.

5 Simulation results

In this section, we present the simulation results to illustrate the performance of the proposed algorithm. We consider a squared target region with side length $L = 500$ m and 10 GUs are randomly located in the region. The bandwidth of each subcarrier is set as $W = 200$ kHz. The channel power at the reference distance of 1 m is set as $\beta_0 = -50$ dB. Each content can be recovered by collecting 4 encoded segments, i.e., $K = 4$, and the size of each encoded segment equals 300 kbits, i.e., $S = 300$ kbits. In addition, the angular speed of the UAV is set as $\alpha = \pi/20$ rad/s.

Figure 2 shows the impact of the flight height on energy efficiency. We compared the proposed algorithm with the Gaussian process based channel prediction algorithm (GPCPA) [15]. As we can see, the energy efficiency decreases with the increase of flight height. Intuitively, higher flight height will increase the distance from the UAV to GUs, thereby reducing the transmission rate of channels and energy efficiency. Moreover, we can find that a higher transmit power can increase energy efficiency. Specifically, a higher transmit power can obtain a higher transmission rate, which can improve the number of bits received by GUs with unit propulsion energy consumption. The propulsion energy consumption is greatly larger than the transmission energy power. Hence, a higher transmit power can increase energy efficiency.

We then compare the low-complexity algorithm with GPCPA in Figure 3, where we plot energy efficiency as a function of the maximum probability of QoS violation ε. As we can see, the increase of ε can improve the energy efficiency of the system. The reason is that a higher ε can make the resource allocation strategy more flexible. Specifically, when ε is small, more subcarriers should be allocated to the GUs with low received rate to ensure that they satisfy the QoS constraints, thereby reducing the energy efficiency. Inversely, when the ε is higher, more subcarriers can be allocated to the GUs with a higher receiving rate. In this case, more QoS violations may occur in the GUs with low received rate, but the energy efficiency of the system will increase.
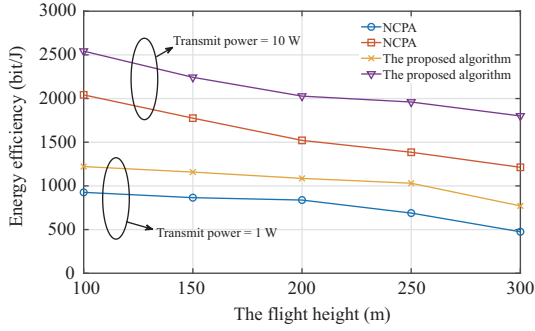
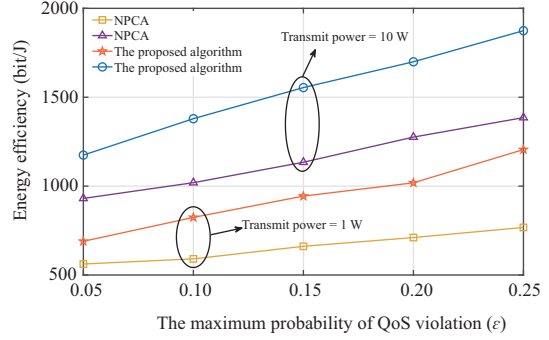**Figure 2** (Color online) The energy efficiency of the UAV versus the flight height.

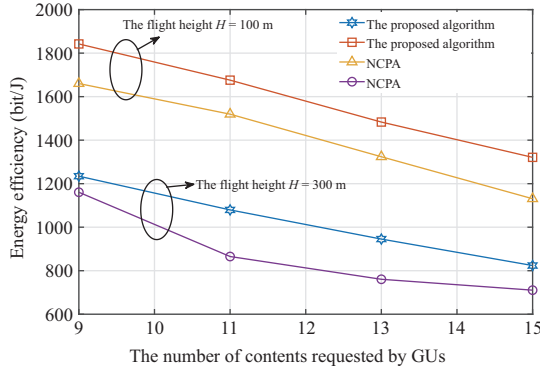**Figure 3** (Color online) The energy efficiency of the UAV versus the maximum probability of QoS violation ε.

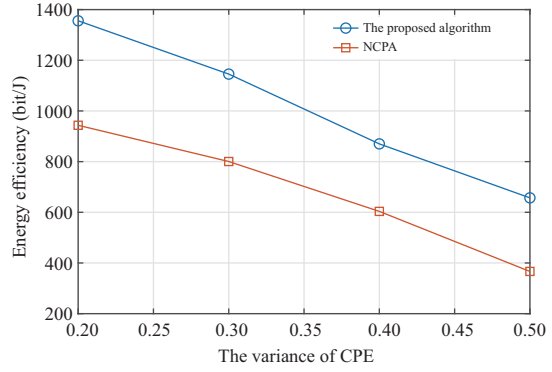**Figure 4** (Color online) The energy efficiency of the UAV versus the QoS constraint (N_{C}).

Figure 5 (Color online) The energy efficiency of the UAV versus the variance of CPE.

The influence of QoS constraint is shown in Figure 4. In particular, a higher QoS constraint of GU refers to the larger number of contents requested by GUs in each flight cycle. We assume that the QoS constraint of each GU is equal. We set the flight height of the UAV as 300 m. The maximum probability of QoS violation is set as 0.1, and the variance of CPE is set as 0.5. As we can see, a higher QoS constraint can decrease the energy efficiency of the system. When the QoS constraint is high, the resource should be more fairly allocated to each GU to ensure the QoS constraint. In this case, GUs with low received rate generally occupy more resource, which decrease the energy efficiency of the system. When the QoS constraint is low, a few subcarriers may guarantee the QoS constraints of the GUs with low received rate. More resources can be allocated to the GUs with high received rate, and further improve the energy efficiency.

In Figure 5, we show the impact of the variance of CPE on energy efficiency. We set the flight height of the UAV as 300 m, and $N_{\mathrm{C}} = 15$. Moreover, the transmit power is set as 1 W, and the maximum probability of QoS violation is set as 0.1. As we can see, a high variance of CPE reduces energy efficiency. The reason is that a higher variance of CPE means a more dispersive distribution of CPE. A more dispersive distribution will generate a larger number of extreme values of CPE. To satisfy the QoS constraint of GU under the extreme value of CPE, the resource allocation strategy will be more conservative. More redundant resource allocation generally occurs in a conservative resource allocation strategy, and further reduces energy efficiency of the system.

6　Conclusion

In this paper, we investigate the TPRA problem in UAV communication networks under imperfect channel prediction. We model the QoS demands of GUs with chance constraints, which are further transformed into deterministic forms with a safe approximation. Then, we prove the transformed optimization programming is convex programming and propose a modified SCA method to optimally solve it. To cater

to the high-speed movement of UAVs, a low-complexity algorithm is tailored. Simulation results show that the proposed low-complexity algorithm generally outperforms GPCPA. Furthermore, the proposed resource allocation can also be applied in other communication systems suffering from the channel prediction error, e.g., the wireless multiple input multiple output relaying system [27], where the system performance will greatly deteriorate if CPE results in the inapposite precoding matrix.

References

1   Zeng Y, Wu Q, Zhang R. Accessing from the sky: a tutorial on UAV communications for 5G and beyond. Proc IEEE, 2019, 107: 2327–2375

2   Gupta L, Jain R, Vaszkun G. Survey of important issues in UAV communication networks. IEEE Commun Surv Tut, 2016, 18: 1123–1152

3   Zhao N, Lu W, Sheng M, et al. UAV-assisted emergency networks in disasters. IEEE Wireless Commun, 2019, 26: 45–51

4   Song Q H, Zeng Y, Xu J, et al. A survey of prototype and experiment for UAV communications. Sci China Inf Sci, 2021, 64: 140301

5   Love D J, Heath R W, Lau V K N, et al. An overview of limited feedback in wireless communication systems. IEEE J Sel Areas Commun, 2008, 26: 1341–1365

6   Jia Z, Sheng M, Li J, et al. LEO-satellite-assisted UAV: joint trajectory and data collection for internet of remote things in 6G aerial access networks. IEEE Internet Things J, 2021, 8: 9814–9826

7   Zeng Y, Zhang R. Energy-efficient UAV communication with trajectory optimization. IEEE Trans Wireless Commun, 2017, 16: 3747–3760

8   Yan S, Peng M, Cao X. A game theory approach for joint access selection and resource allocation in UAV assisted IoT communication networks. IEEE Internet Things J, 2019, 6: 1663–1674

9   Cui F, Cai Y, Qin Z, et al. Multiple access for mobile-UAV enabled networks: joint trajectory design and resource allocation. IEEE Trans Commun, 2019, 67: 4980–4994

10   Zeng F, Hu Z, Xiao Z, et al. Resource allocation and trajectory optimization for QoE provisioning in energy-efficient UAV-enabled wireless networks. IEEE Trans Veh Technol, 2020, 69: 7634–7647

11   Jiang X, Wu Z, Yin Z, et al. Power consumption minimization of UAV relay in NOMA networks. IEEE Wireless Commun Lett, 2020, 9: 666–670

12   Wang B, Sun Y, Zhao N, et al. Learn to coloring: fast response to perturbation in UAV-assisted disaster relief networks. IEEE Trans Veh Technol, 2020, 69: 3505–3509

13   Wang B, Sun Y, Duong T Q, et al. Popular matching for security-enhanced resource allocation in social Internet of flying things. IEEE Trans Commun, 2020, 68: 5087–5101

14   Lu W D, Si P Y, Lu F W, et al. Resource and trajectory optimization in UAV-powered wireless communication system. Sci China Inf Sci, 2021, 64: 140304

15   Ladosz P, Oh H, Zheng G, et al. Gaussian process based channel prediction for communication-relay UAV in urban environments. IEEE Trans Aerosp Electron Syst, 2020, 56: 313–325

16   Zhong X, Guo Y, Li N, et al. Deployment optimization of UAV relay for malfunctioning base station: model-free approaches. IEEE Trans Veh Technol, 2019, 68: 11971–11984

17   Sun Y, Xu D, Ng D W K, et al. Optimal 3D-trajectory design and resource allocation for solar-powered UAV communication systems. IEEE Trans Commun, 2019, 67: 4281–4298

18   Vaezpour E, Dehghan M, Yousefi'zadeh H. Robust joint user association and resource partitioning in heterogeneous cloud RANs with dual connectivity. Comput Commun, 2019, 138: 1–10

19   Liu J, Zhang H, Sheng M, et al. High altitude air-to-ground channel modeling for fixed-wing UAV mounted aerial base stations. IEEE Wireless Commun Lett, 2021, 10: 330–334

20   Zeng Y, Xu J, Zhang R. Energy minimization for wireless communication with rotary-wing UAV. IEEE Trans Wireless Commun, 2019, 18: 2329–2345

21   Dong F, Li L, Lu Z, et al. Energy-efficiency for fixed-wing UAV-enabled data collection and forwarding. In: Proceedings of IEEE International Conference on Communications Workshops (ICC Workshops), 2019. 1–6

22   Nemirovski A. On safe tractable approximations of chance constraints. Eur J Oper Res, 2012, 219: 707–718

23   Garnier J, Omrane A, Rouchdy Y. Asymptotic formulas for the derivatives of probability functions and their Monte Carlo estimations. Eur J Oper Res, 2009, 198: 848–858

24   Geletu A, Klöppel M, Hoffmann A, et al. A tractable approximation of non-convex chance constrained optimization with non-Gaussian uncertainties. Eng Optim, 2015, 47: 495–520

25   Shen K, Yu W. Fractional programming for communication systems-Part I: power control and beamforming. IEEE Trans Signal Process, 2018, 66: 2616–2630

26   Che E, Tuan H D, Nguyen H H. Joint optimization of cooperative beamforming and relay assignment in multi-user wireless relay networks. IEEE Trans Wireless Commun, 2014, 13: 5481–5495

27   Li C, Wang J, Zheng F C, et al. Overhearing-based co-operation for two-cell network with asymmetric uplink-downlink traffics. IEEE Trans Signal Inf Process over Networks, 2016, 2: 350–361